Journal of the Mechanical Behavior of Biomedical Materials 90 (2019) 40–44

Contents lists available at ScienceDirect

Journal of the Mechanical Behavior of Biomedical Materials

journal homepage: www.elsevier.com/locate/jmbbm

Assessment of elastic coefficients of child cortical bone using resonant ultrasound spectroscopy

Marie Semaan[a,c], Pierric Mora[d], Simon Bernard[b], Franck Launay[a,e], Cédric Payan[b], Philippe Lasaygues[b], Martine Pithioux[a,c,*], Cécile Baron[a,c]

[a] Aix-Marseille Univ, CNRS, ISM, Marseille, France
[b] Aix-Marseille Univ, CNRS, Centrale Marseille, LMA, Marseille, France
[c] Aix-Marseille Univ, APHM, CNRS, ISM, Sainte-Marguerite Hospital, Institute for Locomotion, Department of Orthopaedics and Traumatology, Marseille, France
[d] Aix-Marseille Univ., CNRS, IUSTI, Marseille, France
[e] Department of Pediatric Orthopaedic Surgery APHM Timone Hospital, Marseille, France

ARTICLE INFO

Keywords:
Resonant ultrasound spectroscopy
Pediatrics
Cortical bone
Anisotropic elasticity coefficients

ABSTRACT

The assessment of the anisotropic elastic properties of non-pathological child cortical bone remains a challenge for the biomechanical engineering community and an important clinical issue. Resonant ultrasound spectroscopy (RUS) can be used to determine bone stiffness coefficients from the mechanical resonances of bone specimens. Here, a RUS protocol was used on 7 fibula specimens from children (mean age 14 ± 3 years) to estimate the whole elastic stiffness tensor of non-pathological child cortical bone considered as orthotropic. Despite a small number of sample, results are consistent with this hypothesis, even if a trend towards transverse isotropy is discussed. Indeed, the average values of the 9 independent stiffness coefficients obtained in this study for child bone are: C_{11} = 16.73 ± 0.19 GPa, C_{22} = 16.19 ± 0.12 GPa, C_{33} = 24.47 ± 0.30 GPa, C_{44} = 4.14 ± 0.08 GPa, C_{55} = 4.16 ± 0.07 GPa, C_{66} = 3.13 ± 0.05 GPa, C_{12} = 10.14 ± 0.20 GPa, C_{13} = 10.67 ± 0.27 GPa, C_{23} = 10.25 ± 0.14 GPa.

1. Introduction

Bone is a hierarchical and organized structure with properties varying by successive stages from juvenile to mature stage. Currently, Dual Energy X-ray Absorptiometry (DEXA) scanning is the most commonly used bone densitometry method to assess skeletal status in adults and children with bone diseases. Recently, some advances in clinical research assess geometrical and microstructural parameters derived from Computerized Tomography (CT) images. Nevertheless, they not provide measurements of the mechanical characteristics of bone although they have been widely demonstrated to be major determinants of bone quality and fracture risk. Nowadays, using ultrasounds is recognized as a relevant way to provide additional data on the mechanical behavior of bone (Laugier and Haïat, 2011). In the context of mechanical characterization of bone tissue, one of the challenges is to take into account the elastic anisotropy of the material. Indeed, the elastic anisotropy is one of the expressions of physiological adaptation of the bone as a living tissue, and can be a key parameter in the estimation of bone quality. A smart protocol using resonant ultrasound spectroscopy (RUS) has recently been developed to assess the whole stiffness tensor of cortical bone at millimeter scale. The relevant protocol and method are well presented and discussed in the articles by Bernard et al. (2016, 2015, 2013), and recently supplemented by works of Cai et al. (2017). This work, as most of the work conducted on bone, has been carried out on adult bone and more precisely on ageing human bone, which is nowadays a well-documented material. In contrast, cortical bone of children and juveniles remains poorly studied, although it is known to exhibit specific behavior compared with adult bone (Currey and Butler, 1975). Contrary to what has been admitted for years, the mechanical characteristics of child bone cannot be directly deduced from adult bone measurements and require dedicated studies. Nevertheless, child bone pieces are very difficult to collect. The few studies on child bone were conducted on pathological tissue (osteogenesis imperfecta (Albert et al., 2013; Imbert et al., 2014), traumatic brain injury (Davis et al., 2012)). During the last years, pioneer studies have been published on non-pathological child cortical bone (NPCCB) (Bala et al., 2016, 2012a, 2012b; Lefèvre et al., 2015). Lefèvre et al. (2015) measured the diagonal stiffness coefficients of NPCCB (fibula) specimens, which were collected under the same conditions as in the present study (same anatomical site). They provided the values of the

* Correspondence to: Aix-Marseille Université, CNRS, ISM UMR 7287, 13288 Marseille cedex 09, France.
E-mail address: martine.pithioux@univ-amu.fr (M. Pithioux).

https://doi.org/10.1016/j.jmbbm.2018.09.044
Received 13 June 2018; Received in revised form 30 August 2018; Accepted 26 September 2018
Available online 02 October 2018

six diagonal stiffness coefficients, and their statistical sample shows a trend toward transverse isotropy for this kind of material. Unfortunately, the small dimensions of the specimens extracted from the collected pieces prevented the assessment of the off-diagonal coefficients, and the elasticity tensor remained incomplete. This is where the RUS turns out to be a valuable tool.

RUS characterization is fully applicable on low damping materials such as single crystals (Isaak and Ohno, 2003), quasi crystals (Spoor et al., 1995), and metallic composites (Ledbetter et al., 1995). The method has been proved capable of characterizing complex materials such as wood (Longo et al., 2018), rock and concrete (Payan et al., 2007; Remillieux et al., 2015). Also, when combined with a probabilistic approach, it has been able to provide, in a single measurement, the elastic coefficients of specimens of millimetric size of a low-quality factor (Q ~ 20–25) material such as bone (Bernard et al., 2016, 2015).

This case study based on research by Bernard et al., (2016, 2015), is providing the first estimation of the full set of stiffness coefficients of NPCCB initially assumed to be an orthotropic material. Based on our results, we will discuss this hypothesis.

2. Materials and methods

2.1. Specimen preparation

Experiments were conducted on 7 NPCCB specimens extracted from 7 fibulae of children (mean age 14 ± 3 years). The specimens, collected in the distal 1/3 of the fibula, were surgical waste recovered from corrective surgery at the Timone Children's Hospital (*Marseille, France*) after a fracture at the growth plate or *equinovarus* of the foot with no impact on the bone mechanical properties (Rauch et al., 2007). Children were ambulatory prior to surgery and none were under medication known to affect bone modeling or remodeling. Thus, these specimens could be considered as NPCCB specimens. Our experimental protocol respected the legal clauses stated in the French code of Public Health and by the National Commission for Data Protection and Liberties (CNIL-France). Informed consents were obtained from the children legal representatives.

The specimens were cut into rectangular parallelepipeds using a water-cooled low-speed diamond saw (*Buehler Isomet 4000, Buehler, Lake Bluff, IL, USA*). Fig. 1 shows the dimensions along the three directions, radial, circumferential and axial. The geometry of the extracted bone specimens has to be as close as possible to a perfect rectangular parallelepiped in order to conduct the experimental protocol of RUS. Consequently, a specimen holder was specially developed to ensure the parallelism of opposite faces and the perpendicularity of adjacent faces of the bone specimens in the three directions. The proper surface condition of the specimens used in this study was controlled by high-resolution imaging (*Phoenix Nanotom 180 S, General Electric, Germany*). The specimen dimensions were measured using a digital caliper (*Absolute digimatik solar, Mitutoyo, Kanagawa, Japan, measurement error of 0.03 mm*). The area in contact with the sample at the level of the caliper jaws was of the same order of magnitude. The specimen dimensions presented in Table 1 can therefore be considered as average values, whose uncertainty is the one of the caliper. The mass density ρ (in g/cm^3) was determined using a micrometric balance with a density kit (*Voyager 610, Ohaus Corporation, Florham Park, NJ, USA, measurement uncertainty of 0.001 g/cm3*). The fresh specimens were frozen and stored at − 20 °C (Crandall et al., 2000). They were thawed at room temperature, so that during the RUS experiments, measurements were made on fully-hydrated specimens. Freeze-thaw cycles could have a influence on the mechanical properties of bone (Kang et al., 1997). In this work, the number of cycles was limited to only two cycles per sample.

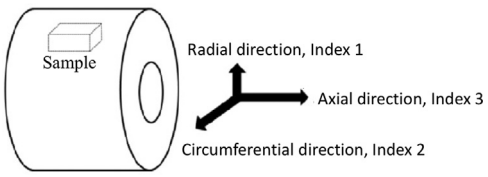

Fig. 1. A sketch representing the bone specimen orientation used in this study.

2.2. Resonant ultrasound spectroscopy (RUS) set-up & protocol

The RUS experiment was conducted in transmission mode using two shear transducers (*V151, Panametrics, Olympus Corporation, Waltham, MA, USA*) facing each other with their axes aligned (Fig. 2), one being used as a transmitter and the other as a receiver (Wang and Lakes, 2003). The bone specimen was placed in between. The center frequency was 500 kHz, with a frequency bandwidth from 60 to 800 kHz.

A waveform generator (*PXI-5406, National Instrument, Austin, Texas, USA*) was used to produce a constant amplitude stepped sine wave. The transmitted signal was amplified by a high voltage amplifier (*WMA-30NN, Falco Systems BV Remisestraat 1 2225 TH Katwijkaan Zee, The Netherlands*). The resulting vibrating signal was recorded using an A/D converter (*PXI-5122 A/D, National Instrument, Austin, Texas, USA*). The signal processing algorithms were implemented on an ordinary personal computer, using Matlab (The MathWorks, Inc., Natick, Massachusetts, United States) and Python (2001–2018 Python Software Foundation).

The RUS method is a method for measuring the stiffness coefficients C_{ij} following Hooke's law (Migliori et al., 1993). The method is based on the excitation of the natural vibrational modes of a specimen and the measurement of the spectrum resonance peaks. The general protocol is divided into 3 steps.

The first step is to estimate theoretical resonant frequencies from the measurement of the dimensions and mass of the bone specimen and an initial guessed value of the elasticity tensor. In this work, we considered NPCCB as orthotropic and we then had to evaluate 9 stiffness coefficients. As a result, the frequency range to be considered was defined so as to enclose 30 resonant frequencies for each specimen. The initial values of the coefficients of the presumed elasticity tensor were the six diagonal coefficients values published in (Lefèvre et al., 2015) (Table 1). The three off-diagonal coefficients were supposed to be equal and deduced from

$$C_{12} = C_{13} = C_{23} = C_{11} - 2C_{66} = 10.24GPa.$$

The second step is the excitation of the specimen over the theoretical frequency range obtained in the first step. The measurement RUS protocol requires free surface boundary conditions (Migliori and Maynard, 2005). Our specimens were rectangular parallelepipeds. The contact surface with the transducers was reduced to its corners (Fig. 2) whose symmetry was low so that there would be no vibration node there. This position allows all natural modes to be excited and a maximum number of frequencies to be measured.

Both generated and stored signals were managed using RITA (Resonance Inspection Techniques and Analyses) software, designed and implemented by the LANL Wave Physics group (Payan et al., 2014; Remillieux et al., 2015). Measurements were repeated and the specimen removed and repositioned 6 times, so as to detect the maximum number of resonant frequencies (Fig. 3). This repositioning can lead to slight variations in coupling between the transducers and the specimen, and increases the possibility of obtaining weakly excited modes. Repeated measurements reduce the number of missed modes and are a way of estimating the uncertainty on resonant modes. Total bone specimen testing time was roughly 30 min.

The third step is the detection of the actual resonant frequencies, and the resolution of the inverse problem on identifying the stiffness coefficients. The positions of the peaks in the modulus spectra were detected using the "peak-finder" option of the RITA software. Once the local maxima are identified, a parabolic fit is performed over the few

Table 1
Values, mean and standard deviation (SD) of sizes, densities and measured stiffness coefficients, elastic moduli, shear moduli and Poisson's ratios for seven child fibula samples. All coefficients except Poisson's ratios are in GPa.

Age	9 y. o.	11 y. o.	13 y. o.	14 y. o.	15 y. o.	16 y. o.	18 y. o.	Mean	SD
Size (mm) radial x circumferential x axial	1.2 × 2.4 × 4.1	1.5 × 4.6 × 4.4	1.8 × 3.3 × 6.2	1.1 × 2.7 × 5.6	2.4 × 2.6 × 3.5	1.4 × 4.3 × 6.2	1 × 1.3 × 4.1	–	–
Volume (mm^3)	12	30	37	17	22	37	5	–	–
Density ρ (g/cm^3)	2.52	2.02	2.04	2.24	2.21	1.96	1.97	**2.14**	**0.20**
C_{11}	16.86	16.5	16.59	16.99	16.85	16.79	16.51	**16.73**	**0.19**
C_{22}	16.25	16.3	16.14	16.08	16.12	16.06	16.37	**16.19**	**0.12**
C_{33}	24.4	24.5	25.06	24.47	24.16	24.2	24.53	**24.47**	**0.30**
C_{44}	4.21	4.2	3.99	4.1	4.17	4.12	4.22	**4.14**	**0.08**
C_{55}	4.18	4.1	4.19	4.3	4.09	4.16	4.09	**4.16**	**0.08**
C_{66}	3.19	3.2	3.06	3.1	3.21	3.14	3.14	**3.15**	**0.06**
C_{12}	10.18	10	10.14	10.06	10.5	9.84	10.24	**10.14**	**0.21**
C_{13}	11.15	10.5	10.5	10.86	10.49	10.42	10.79	**10.67**	**0.27**
C_{23}	10.28	10.4	10.14	10.32	10.47	10.09	10.13	**10.26**	**0.15**
E_1	9.2	9.4	9.3	9.6	9.2	9.8	9.0	**9.36**	**0.27**
E_2	9.4	9.3	9.2	9.3	8.7	9.4	9.3	**9.23**	**0.24**
E_3	15.8	16.2	17	16	16	16.2	16.3	**16.21**	**0.38**
G_{12}	3.19	3.2	3.06	3.1	3.21	3.14	3.14	**3.15**	**0.06**
G_{13}	4.18	4.1	4.19	4.3	4.09	4.16	4.09	**4.16**	**0.08**
G_{23}	4.21	4.2	3.99	4.1	4.17	4.12	4.22	**4.14**	**0.08**
ν_{12}	0.46	0.47	0.49	0.47	0.51	0.46	0.47	**0.48**	**0.02**
ν_{13}	0.26	0.23	0.22	0.25	0.21	0.24	0.24	**0.24**	**0.01**
ν_{23}	0.21	0.23	0.20	0.22	0.22	0.22	0.20	**0.21**	**0.01**
ν_{21}	0.47	0.46	0.48	0.45	0.48	0.45	0.49	**0.47**	**0.01**
ν_{31}	0.45	0.40	0.40	0.41	0.37	0.39	0.44	**0.41**	**0.02**
ν_{32}	0.35	0.39	0.37	0.38	0.41	0.39	0.34	**0.38**	**0.02**

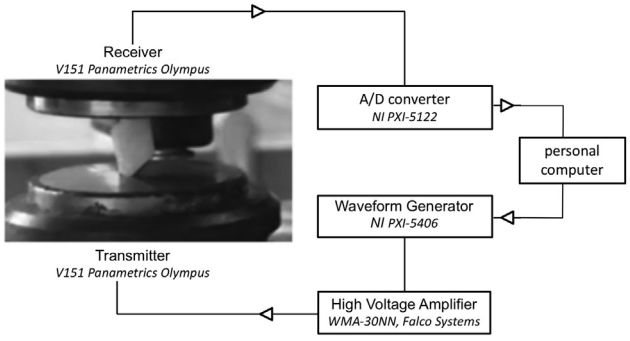

Fig. 2. Photograph of the bone specimen inserted between the two transducers. Scheme of the electroacoustic setup.

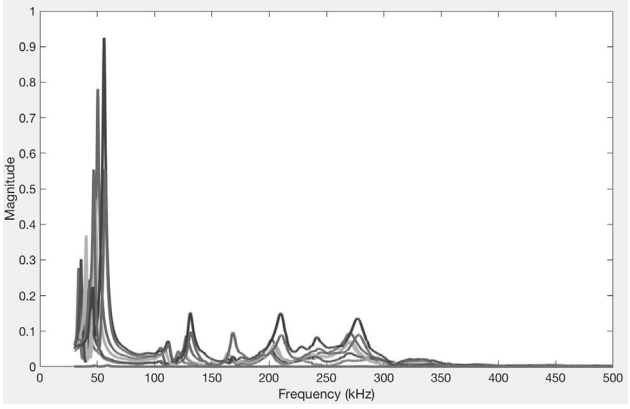

Fig. 3. Typical set of spectra measured for a NPCCB specimen (13 y. o.). Each curve corresponds to one of the 6 repeated measurements (sample removed and repositioned).

points close to the max to increase the frequency resolution. Among these peaks, the user selected those which correspond to a phase shift. Details can be found in Payan et al. (2014). However, due to the low-quality factor of cortical bone material, the resonant peaks obtained experimentally were often overlapped and were difficult to detect, leading to missed resonant modes. Moreover, it is tricky to obtain the right pairing between experimental and theoretical modes. To tackle these issues, we implemented the Bayesian approach described in Bernard et al. (2015). The Bayesian inference is a subjective probabilistic model which integrates prior information on the parameters. Then it estimates the likelihood of a set of parameters to obtain the data. In our case, however, existing knowledge of the parameters could not easily be translated into probability distributions, so we used Gibbs sampling to randomly explore the posterior probability density function following a Markov Chain Monte Carlo method. Details can be found in Bernard et al. (2015).

3. Results and discussion

The stiffness coefficients C_{ij} were calculated after 300 iterations, related to the convergence of the Markov chains from the values obtained over 1000 random statistical samples (Gibbs sampling). These elastic constants are also translated in terms of elastic moduli E_i, shear moduli G_{ij} and Poisson's ratios ν_{ij} (i, j = 1, 2, 3 for radial, circumferential and axial directions). The experimental protocol (holding of the sample, transducers location, etc.) was carefully validated on comparable size aluminum samples. Following this protocol, all of the spectra were used to enhance the detection of resonant frequencies over the 6 independent measurements performed for each sample. No prior judgment was assumed related to the quality of the measurement.

Results for bones are presented in Table 1 and Table 2. Table 2 presents the stiffness coefficients of adult and child cortical bones obtained by Bernard et al. (2016), Lefèvre et al. (2015), and in this case study. Lefèvre et al. (2015) evaluated only the diagonal stiffness coefficients for the NPCCB while Bernard et al. (2016) evaluated the whole stiffness matrix for adult cortical tibia specimens with millimetric dimensions comparable to the dimensions of the present NPCCB specimens (from 5 to 37 mm^3).

The diagonal stiffness coefficients for child bone are consistent with those obtained by Lefèvre *et al.*, with differences $\left(\frac{\delta x}{x}\right)$ ranging from 0.6% (C_{44} and C_{66}) to 2.71% (C_{55}). The measured coefficients for child

Table 2
Mean stiffness coefficients of adult and child cortical bones (all values in GPa).

Stiffness coefficients	Bernard et al. (2016) (Bernard et al., 2016)	Lefèvre et al. (2015) (Lefèvre et al., 2015)	Semaan et al. (2018) Present study
Type of specimens	Adult tibia	Child fibula	Child fibula
C_{11}	14.79 (3.39)*	16.5	16.73 (0.19)*
C_{22}	14.79 (3.39)*	15.8	16.19 (0.12)*
C_{33}	26.64 (3.48)*	24	24.47 (0.3)*
C_{44}	5.52 (1.05)*	4.17	4.14 (0.08)*
C_{55}	5.52 (1.05)*	4.05	4.16 (0.07)*
C_{66}	3.65 (0.9)*	3.13	3.15 (0.05)*
C_{12}	7.49 (1.6)*	–	10.14 (0.2)*
C_{13}	8.31 (1.01)*	–	10.67 (0.27)*
C_{23}	8.31 (1.01)*	–	10.26 (0.14)*

* = mean (standard deviation).

bone are lower than for adult bone. The relative differences range from 8.1% (C_{33}) to 35% (C_{12}). For the adult bone values presented in Table 2, the hypothesis chosen by Bernard et al. (2016) is transverse isotropy; commonly assumed for the adult long bone cortex. The stiffness coefficients C_{11} and C_{22} (respectively C_{55} and C_{44}) are then identical.

In the analysis of our results, coefficients C_{11} and C_{22} are on average close to each other; equal to 16.73 GPa and 16.19 GPa, with a relative difference of 3.22%. The coefficients C_{44} and C_{55} can be considered as identical, equal to 4.14 GPa and 4.16 GPa, with a relative difference of 0.5%.

Due to the scarcity and the small dimensions of specimens, working on NPCCB is challenging. The preparation (cutting and cleaning) of the samples remains a delicate step in the experimental protocol to provide satisfying geometry and surface quality (roughness and flatness) of the sample. Moreover, an important criterion in the RUS protocol is the parallelism of the specimen (Migliori and Maynard, 2005). It is important to have a rectangular parallelepiped specimen as perfect as possible without pores on faces, edges and corners. Even using a specially-designed specimen holder, some of our specimens showed open pores at the boundaries, thus compromising the flatness of the faces and the correspondence between the theoretical and experimental resonant frequencies. Such specimens were removed after high-resolution imaging control using an X-ray scanner, which further reduced the number of specimens available. The low number of specimens was thus an important limitation in this work. It prevented any statistical analysis of the relationship between age and stiffness coefficients or of the degree of anisotropy of NPCCB specimens (orthotropic versus transversely isotropic material).

Following the orthotropy hypothesis, the inverse problem should provide 9 independent elastic coefficients. According to Lebedev's work (Lebedev, 2002), the number of modes to measure should be equal to 5 times the number of coefficients to calculate. That is 45 modes in our case. Given our assumptions introduced in the first step, the theoretical frequency range encloses the 30 first modes. But due to the low-quality factor of bone material, the detection of each of the 30 modes was not always possible. The minimum number of frequencies identified for a specimen was 21. However, following the work of Bernard et al., (2016, 2015), we used the Bayesian approach to circumvent this problem and to solve the inverse problem of calculating stiffness coefficients from a number of resonant frequencies lower than 5 times the number of coefficients to calculate and with a minimal error (Cai et al., 2017).

Despite a small number of samples and statistical values, results are consistent with the orthotropic hypothesis for NPCCB specimens studied in this work. But the results also show a trend towards transverse isotropy for this kind of material, which should be confirmed using a representative statistical sample. However, the low number of specimens precludes making statistical analysis on the significance of the differences between C_{11} and C_{22}, C_{44} and C_{55}, and C_{13} and C_{23}. This hypothesis warrants further investigation, by considering NPCCB as a transversely isotropic material in the forward problem (step 1). Regarding the operational conditions (low sample count, possible number of thawing cycles, limited number of tests), and with no certainty on the degree of anisotropy, the most general case of orthotropy was retained in this study.

4. Conclusions

The assessment of the complete elastic stiffness tensor of non-pathological child cortical bone (NPCCB) remains challenging and critical needs for the biomechanics community. Although relevant studies exist, bibliographic references are relatively rare, and few studies focus on NPCCB. In this work, we present values for NPCCB elastic coefficients at millimeter scale, obtained from Resonant ultrasound spectroscopy (RUS) measurements. RUS has been demonstrated to be suitable for the evaluation of bone elasticity, in particular by the work of Bernard *et al.*, from which this study is strongly inspired. This work is a case study of the use of RUS for NPCCB characterization. Although it has been conducted on a small number of specimens, this study is the first, to our knowledge, to provide a complete elastic stiffness tensor for NPCCB. These values obtained at millimeter scale can be crucial to implement homogenization methods to assess macroscopic properties and develop realistic numerical child bone models.

Acknowledgments

We are grateful to the donors or their legal representatives. This work benefited from the help of Eric Debieu, Vincent Long, Clémentine Boullai, Magali Gaiani and Angela D'Arienzo in setting up experiments. We thank Claude-Hélène Mignard for English language revision.

Funding sources

This work was funded by Aix-Marseille University, Erasmus Mundus HERMES program, and the STAR Carnot Institute.

Declarations of interest

None.

References

Albert, C., Jameson, J., Toth, J.M., Smith, P., Harris, G., 2013. Bone properties by nanoindentation in mild and severe osteogenesis imperfecta. Clin. Biomech. 28 (1), 110–116.

Bala, Y., Lefèvre, E., Roux, J.P., Baron, C., Lasaygues, P., Pithioux, M., Kaftandjian, V., Follet, H., 2016. Pore network microarchitecture influences human cortical bone elasticity during growth and aging. J. Mech. Behav. Biomed. Mater. 63, 164–173.

Bernard, S., Grimal, Q., Laugier, P., 2013. Accurate measurement of cortical bone elasticity tensor with resonant ultrasound spectroscopy. J. Mech. Behav. Biomed. Mater. 18, 12–19.

Bernard, S., Marrelec, G., Laugier, P., Grimal, Q., 2015. Bayesian normal modes identification and estimation of elastic coefficients in resonant ultrasound spectroscopy. Inverse Probl. 31 (6), 065010.

Bernard, S., Schneider, J., Varga, P., Laugier, P., Raum, K., Grimal, Q., 2016. Elasticity–density and viscoelasticity–density relationships at the tibia mid-diaphysis assessed from resonant ultrasound spectroscopy measurements. Biomech. Model. Mechanobiol. 15 (1), 97–109.

Berteau, J.P., Baron, C., Pithioux, M., Chabrand, P., Lasaygues, P., 2012a. Mechanical properties of children cortical bone: a bimodal characterization. in Mechanical properties of children cortical bone: A bimodal characterization, Nantes, France, pp. 1–5.

Berteau, J.P., Pithioux, M., Baron, C., Gineyts, E., Follet, H., Lasaygues, P., Chabrand, P., 2012b. Characterisation of the difference in fracture mechanics between children and adult cortical bone. Comput. Methods Biomech. Biomed. Eng. 15 (supp1), 281–282.

Cai, X., Peralta, L., Gouttenoire, P.J., Olivier, C., Peyrin, F., Laugier, P., Grimal, Q., 2017. Quantification of stiffness measurement errors in resonant ultrasound spectroscopy of human cortical bone. J. Acoust. Soc. Am. 142 (5), 2755–2765.

Crandall, K., Bininda-Emonds, O., Mace, G., Wayne, R., 2000. Considering evolutionary processes in conservation biology. Trends Ecol. Evol. 15 (7), 290–295.

Currey, J.D., Butler, G., 1975. The mechanical properties of bone tissue in children. J.

Bone Jt. Surg. Am. 57 (6), 810–814.
Davis, M.T., Loyd, A.M., Shen, H.H., Mulroy, M.H., Nightingale, R.W., Myers, B.S., Bass, C.D., 2012. The mechanical and morphological properties of 6 year-old cranial bone. J. Biomech. 45 (15), 2493–2498.
Imbert, L., Aurégan, J.C., Pernelle, K., Hoc, T., 2014. Mechanical and mineral properties of osteogenesis imperfecta human bones at the tissue level. Bone 65, 18–24.
Isaak, D.G., Ohno, I., 2003. Elastic constants of chrome-diopside: application of resonant ultrasound spectroscopy to monoclinic single-crystals. Phys. Chem. Miner. 30 (7), 430–439.
Kang, Q., An, Y.H., Friedman, R.J., 1997. Effects of multiple freezing-thawing cycles on ultimate indentation load and stiffness of bovine cancellous bone. Am. J. Vet. Res. 58 (10), 1171–1173.
Laugier, P., Haïat, G., 2011. Bone Quantitative Ultrasound. Springer Science, New York, Dordrecht.
Lebedev, A.V., 2002. Method of linear prediction in the ultrasonic spectroscopy of rock. Acoust. Phys. 48 (3), 339–346.
Ledbetter, H., Fortunko, C., Heyliger, P., 1995. Orthotropic elastic constants of a boron-aluminum fiber-reinforced composite: an acoustic-resonance-spectroscopy study. J. Appl. Phys. 78 (3), 1542–1546.
Lefèvre, E., Lasaygues, P., Baron, C., Payan, C., Launay, F., Follet, H., Pithioux, M., 2015. Analyzing the anisotropic Hooke's law for children's cortical bone. J. Mech. Behav. Biomed. Mater. 49, 370–377.
Longo, R., Laux, D., Pagano, S., Delaunay, T., Le Clézio, E., Arnould, O., 2018. Elastic characterization of wood by Resonant Ultrasound Spectroscopy (RUS): a comprehensive study. Wood Sci. Technol. 52 (2), 383–402.
Migliori, A., Sarrao, J.L., Visscher, W.M., Bell, T.M., Lei, M., Fisk, Z., Leisure, R.G., 1993. Resonant ultrasound spectroscopic techniques for measurement of the elastic moduli of solids. Phys. B Condens. Matter 183, 1–24.
Migliori, A., Maynard, J.D., 2005. Implementation of a modern resonant ultrasound spectroscopy system for the measurement of the elastic moduli of small solid specimens. Rev. Sci. Instrum. 76 (12), 121301.
Payan, C., Garnier, V., Moysan, J., Johnson, P.A., 2007. Applying nonlinear resonant ultrasound spectroscopy to improving thermal damage assessment in concrete. J. Acoust. Soc. Am. 121 (4), EL125–EL130.
Payan, C., Ulrich, T.J., Le Bas, P.Y., Saleh, T., Guimaraes, M., 2014. Quantitative linear and nonlinear resonance inspection techniques and analysis for material characterization: application to concrete thermal damage. J. Acoust. Soc. Am. 136 (2), 537–546.
Rauch, F., Travers, R., Glorieux, F.H., 2007. Intracortical remodeling during human bone development—A histomorphometric study. Bone 40 (2), 274–280.
Remillieux, M.C., Ulrich, T.J., Payan, C., Rivière, J., Lake, C.R., Le Bas, P.Y., 2015. Resonant ultrasound spectroscopy for materials with high damping and samples of arbitrary geometry: rus for arbitrary shape and high damping. J. Geophys. Res. Solid Earth. 120 (7), 4898–4916.
Spoor, P.S., Maynard, J.D., Kortan, A.R., 1995. Elastic isotropy and anisotropy in quasicrystalline and cubic AlCuLi. Phys. Rev. Lett. 75 (19), 3462–3465.
Wang, Y.C., Lakes, R.S., 2003. Resonant ultrasound spectroscopy in shear mode. Rev. Sci. Instrum. 74 (3), 1371–1373.